University of Baghdad
College of Engineering
JOURNAL OF ENGINEERING

Journal of Engineering
journal homepage: www.jcoeng.edu.iq
Volume 31 Number 8 August 2025

Performance Analysis of the Stilling Basin of the Taziz Al-Taziz Pumping Station in Al-Muthanna Governorate, Iraq

Arafh Fadhel Albayati *, Riyadh Z. Azzubaidi

Department of Water Resources, College of Engineering, University of Baghdad, Baghdad, Iraq

ABSTRACT

Taziz Al-Taziz irrigation pumping station, within Al-Muthanna Governorate, Iraq, was studied, aiming at investigating the performance of its stilling basin in reducing the energy of the water out of the discharge pipes outlet. The study relied on the results of the physical model of the basic design of the stilling basin and the use of ANSYS Fluent 21.0 software to simulate both the basic design and the as-built stilling basin. The physical model was constructed and studied by the Center for Studies and Engineering Designs of the Iraqi Ministry of Water Resources. Simulations showed the variation in velocity within the basic design of Taziz Al-Taziz pumping station to be 3.98 m/s to 0.209 m/s in the basin, with an average velocity at the beginning of the canal of 1.4 m/s. For that, as built Taziz Al-Taziz, the velocity results showed a variation of 3 m/s to 0.209 m/s within the basin with an average velocity of 1m/s at the beginning of the canal. By converting the physical model's measured results to a prototype, the average velocity at the beginning of the canal is 1.28 m/s. The efficiency of the basic design stilling basin is 30.7%, while that for the as-built is 50.5 % and 36.7% for the physical model. This indicates the quality and efficiency of the as-built stilling basin in dispersing a significant percentage of water energy from the pipes. Moreover, it was found that no negative pressure is developed within the basins.

Keywords: Stilling basin, ANSYS fluent, Hydraulic design, Velocity distribution, Pumping station, Coupled algorithms.

1. INTRODUCTION

Stilling basins are hydraulic structures that are used to reduce the velocity of water flowing from pipe outlets and to reduce its energy before it reaches the canal. This process protects the bed and sides of the canal from corrosion. The General Authority for Irrigation Projects Operation of the Iraqi Ministry of Water Resources has a problem in one of its irrigation pumping stations. This station is known as Taziz Al-Taziz Irrigation Pumping Station, located within Al-Muthanna Governorate. The stilling basin of this pumping station reached its

*Corresponding author
Peer review under the responsibility of University of Baghdad.
https://doi.org/10.31026/j.eng.2025.08.10

Article received: 26/02/2025
Article revised: 13/04/2025
Article accepted: 30/05/2025
Article published: 01/08/2025

maximum water level, and high velocities were noticed at the downstream side of the basin. Numerous studies on hydraulic performance and water flow have been completed over the years.

(Behnamtalab et al., 2023) focused his study on how the United States Bureau of Reclamation USBR VI stilling basin works in dispersing the energy of turbulence by analyzing various flow characteristics, including average and maximum velocities, turbulent dissipation rates, and turbulent kinetic energy. The goal is to investigate the effects of two key parameters, Froude number Fr and the width-to-depth ratio (W/D), on the flow characteristics within the USBR VI stilling basin. The researchers used numerical simulations to monitor the turbulent flow characteristics in the USBR VI stilling basin by using 3D Flow software and FVM to solve the equations. They specifically used the RNG k-ε turbulence model. They looked at the velocity profiles and pressure measurements to validate their findings, achieving a close match with an average error of about 1.2%. The W/D ratio from 3.50 to 9.23 significantly affects the flow characteristics in the USBR VI stilling basin. Similarly, the maximum velocity reduction at the end of the basin increases from 40% to 87% as W/D increases.

(Zaffar and Hassan, 2023) examined the hydraulic performance of the stilling basins at Taunsa Barrage, with a particular emphasis on how design modifications impact their effectiveness. Comparing the basins before and after they were remodeled is part of this. Uses AutoCAD to create the stilling basin designs and FLOW-3D to simulate three-dimensional fluid flow using the finite volume approach. When it came to energy dissipation, they discovered that the old stilling basin performed better than the new one, and the old stilling basin's initial Froude number (Fr) decreased as the tailwater increased, and the new basin's maximum efficiency was approximately 55%. In contrast, the old basin hydraulic jump efficiency was higher, reaching up to 56% at specific tailwater levels. On the other hand, in the new stilling basin, when tailwater levels rose, so did the Froude number and the subsequent depths, and this suggested a more turbulent flow, which dissipated energy less effectively.

(Sharma et al., 2021) refer to assessing how well the impact stilling basin functions in dissipating energy from flowing water, and the simulations are executed in Fluent R15.0 to develop a three-dimensional model of the impact stilling basin using ANSYS Workbench and analyze the performance of the impact stilling basin in different scenarios and the simulations revealed that the maximum energy dissipation occurs when the baffle wall is positioned at a distance of 4d from the inlet and 1d from the floor, 'd' is defined as the equivalent diameter of the pipe outlet and the research confirms that the impact stilling basin is effective in dissipating energy from flowing water, the placement of the baffle wall significantly influences the energy dissipation process, which is crucial for preventing erosion and scouring downstream.

(Mohammed et al., 2020) aimed at increasing the energy dissipation, lowering downstream flow velocity, and developing a design of stilling basins used in sewage networks to keep the outlet structures from eroding and scouring. The study applied the numerical simulation techniques in FLOW-3D to determine the best stilling basin designs by adjusting variables, including the Froude number, intake pipe height, and the shape and arrangement of dissipators. After testing six distinct disperser shapes, the optimal model was chosen based on the greatest energy dissipation ratio (ΔE/E1), which ranged greatly between 16% and 85%. As the Froude number (Fr) rose, the energy dissipation ratio improved, and they discovered that the turbulent energy dissipation ratio (ΔE/E1) changed

dramatically, suggesting that the stilling basins' layout and design had a considerable impact on their performance.

(Babaali et al., 2019) tried to improve the energy dissipation in stilling basins, particularly in cases of discharges exceeding design capacity. An adverse slope is introduced at the end of (USBRII) stilling basin in the Nazloochay dam model and the study employs a combination of numerical simulations using Flow-3D software and experimental data to investigate various hydraulic parameters and these parameters include pressure distribution, Froude number, water surface profile, air entrainment, and turbulent dissipation, particularly for a discharge rate of 300 m^3/s and the research confirms the accuracy of the numerical model by comparing it with experimental data. It highlights the effectiveness of the numerical model, with a particular emphasis on the results obtained using the RNG turbulence model, and the study also provides insights into the variations in turbulent dissipation along the length of the stilling basin. Overall, this research aims to enhance the hydraulic performance of stilling basins, contributing to practical applications in the field of hydraulic engineering.

(Soori et al., 2017) Suggests enhancing the design of particular structures at the USBR II stilling basin type, and the primary objective of the research is to determine the appropriate arrangement for the inlet and outlet barriers at the USBR II stilling basin to enhance their ability to regulate water flow and dissipate energy. Using Flow-3D software to simulate the flow, the researchers examine several barrier designs, including variations in height and thickness, to ascertain which arrangement is most effective for discharges of 830 m^3/s. According to the findings, the highest performance was obtained when barriers that were one and a half meters high were used, together with three steps at the stilling basin edge.

(Valero et al., 2016) examined the flow in a USBR II stilling basin, especially when discharge levels were higher than those for which the basin was initially intended. A computational fluid dynamics CFD model was created for simulations, and a reduced-scale physical model was built for tests. Using numerical and physical models, the study effectively reproduced the hydraulic jump form, velocity profiles, and pressure distributions seen in the USBR II stilling basin.

(Babaali et al., 2015) investigated the hydraulic jump in a convergence stilling basin, particularly the USBR II basin at the Nazloo Dam in Iran and the research uses a numerical model, specifically the FLOW-3D software, to simulate the hydraulic conditions and the study employs two turbulence models, k-ε and RNG, and compares their results with physical model data and the numerical model accurately predicts parameters like velocity, pressure, Froude numbers, air entrainment, and hydraulic jump efficiency and the findings suggest that the basin with converged walls performs better in creating hydraulic jumps than parallel walls and the study highlights the effectiveness of numerical modeling as a cost-effective alternative to physical models for assessing hydraulic jump behavior in stilling basins and the RNG turbulence model, in combination with the volume-of-fluid (VOF) surface tracking method, provides accurate results for 3D fluid motion patterns.

(Peterka, 1964; Aleyasin et al., 2015) specified the particular design of the stilling basin being studied, and type VI refers to a classification used by the USBR indicating a specific geometry and function, and the term "short impact" implies that the basin is designed to handle flows with a short hydraulic jump, which is crucial for energy dissipation. By analyzing and improving how effectively the Type VI short impact stilling basin dissipates energy from turbulent flows and the research involves measuring flow velocities at various locations within the basin under different Froude numbers. And compares the performance of the standard USBR VI basin with modified configurations that include various splitter

types and baffle placements. Strong vortices were observed both upstream and downstream of the impact baffle during tests, and these vortices play a significant role in dissipating kinetic energy from the flow, which is essential for reducing turbulence and potential scouring downstream. The study provided quantitative data on streamwise velocities across various tests. It was found that the local velocities varied, with lower velocities at certain points indicating effective energy dissipation, and the results also showed that maintaining a balance in flow rates is crucial for the basin efficiency, and the combination of cellular baffles and flow splitters significantly improves the dissipation of kinetic energy in the stilling basin. Specifically, splitter type 2 was identified as the most effective in achieving calm flow and reducing turbulence.

(Tabatabai et al., 2014) Investigated stilling basins with a sinusoidal bed shape by examining the flow characteristics of a stilling basin by the uses of a computational fluid dynamics program called Flow 3D to simulate and illustrate the flow patterns and the channel used for the testing had dimensions of 12, 3.0, and 4.0 for length, width, and height, respectively and the height of sinusoidal bumps is 10, 20, and 30 mm, and their wavelength is 40 mm. In this study, the range of Froude numbers is 4.6 to 12.2, and this method enables a thorough examination of how the bed's sinusoidal form affects water circulation, and the simulations reveal different flow patterns driven by the sinusoidal bed form. Variations in velocity and turbulence levels are among these patterns. Higher turbulence can improve mixing and energy dissipation, two processes that are critical to stilling basin performance and the study concludes that both physical and numerical modeling techniques are useful for examining the flow in USBR II stilling basins, especially when discharge levels are greater than those for which the basin was initially intended and the capacity to adjust is essential for comprehending and enhancing your performance.

(Aboul Atta et al., 2011) Presented a new baffle rough shape called the T-shape instead of the conventional cubic form, and to improve stilling basin design, which is utilized to disperse water flow energy and stop erosion downstream. Involves testing the effectiveness of a novel T-shaped roughness design in stilling basins through experiments in a hydraulic laboratory. When compared to a smooth bed, T-shape roughness drastically shortens the hydraulic leap. Between 7.2% to 8.8% is the ideal roughness intensity found for increasing energy loss and reducing jump duration. For the intended hydraulic performance to be achieved, this range is essential.

(Lu et al., 2008) Combined advanced numerical techniques to simulate complex fluid dynamics involving turbulence and free surfaces, particularly in scenarios where the flow encounters obstacles and they propose a two-dimensional hybrid numerical model, named FEM-LES-VOF, which integrates the finite element method (FEM), large eddy simulation (LES), and the Computational Lagrangian-Eulerian Advection Remap Volume of Fluid (CLEAR-VOF) method and the model is designed to effectively simulate turbulent free surface flows that involve violent interactions and complex boundary configurations and the results indicated that turbulence and vortex structures significantly influence the evolution of reflection waves in free surface flows. The results from the FEM-LES-VOF model were found to be in good agreement with previous numerical predictions, particularly in the later stages of free surface evolution, and the study successfully developed a numerical model for simulating turbulent free surface flow, combining the three-step Taylor-Galerkin finite element method, large eddy simulation (LES), and the CLEAR-VOF method.

(Goel, 2007) conducted a real-world trials carried out in a lab environment and the main objective is to suggest new stilling basin designs that are shorter and more effective than the

ones that are already in use, particularly the USBR type VI stilling basin and the purpose of the study is to perform laboratory tests on models that have a 4 cm × 4 cm square aperture and the stilling basin model length might be decreased from 12.9 times their diameter (12.9 d) to 10.9 times (10.9 d) and this indicates a more compact and effective design since it represents a decrease of almost 15% when compared to the USBR type VI stilling basin model. Effective hydraulic performance may be achieved with a more compact design, as seen by the stilling basin model's decreased length.

All of the above were laboratory experiments and field observations. Computer simulations were used in various studies on different stilling basins with different dimensions and designs to study and analyze the behavior of water and energy dissipation mechanics and their downstream effects. This study uses the numerical method to analyze the behavior of water pipe outlets. This study aims to Develop and verify a comprehensive mathematical model by using the ANSYS Fluent 21.0 software, which combines pressure and velocity techniques with an emphasis on pressure-based and momentum-coupled algorithms with applied the k-ε turbulent model and finite volume method VOF to simulate the water flow and using the developed model to investigate and analyze the hydraulics of the flow and the energy dissipation mechanisms within stilling basins. The results of the mathematical model will be compared to the physical model designed by the Center for Studies and Engineering Designs. A comprehensive investigation can help create designs that enhance sustainability and performance.

2. DESCRIPTION OF THE STILLING BASINS

According to data from **(Center of Studies and Engineering Designs, 2024)**. The stilling basin of the Taziz Al-Taziz pumping station is shown in **Fig. 1**. It has a dimension of 8 m in length, 12 m in width, and 5 m in height, with top and bed levels 18.3 and 13.3 m.a.m.s.l. Respectively. Three operational pipes with a diameter of 1.6 m and one standby pipe discharging a maximum of 15 m^3/s.

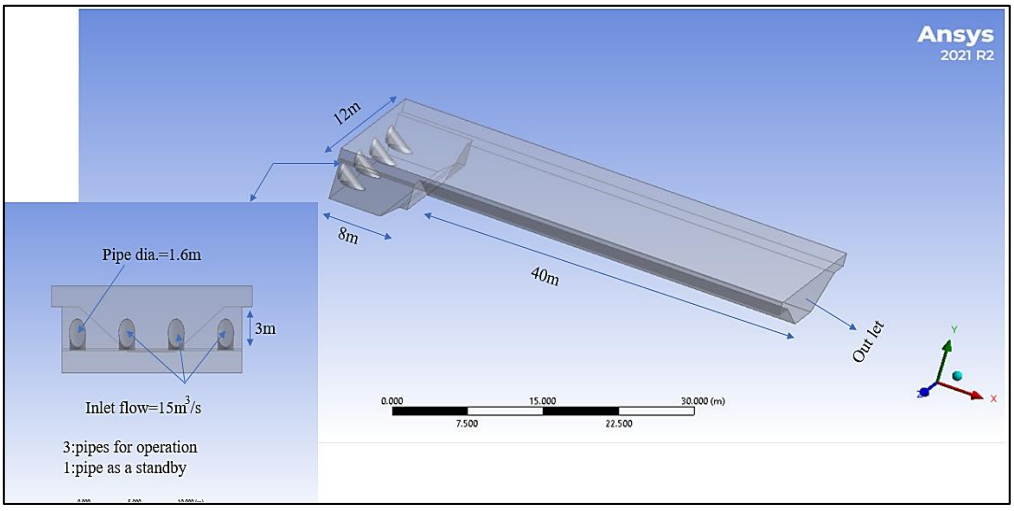

Figure 1. Geometry of the basic design of the stilling basin.

By knowing the distance of the pipe opening from the retaining wall and the height of the wall, the angle of inclination of the pipe inside the basin was calculated to be 36°, and the height of the pipe opening from the bed of the stilling basin is 1m. The basin is connected to

a main irrigation canal designed with a 4.75 m bed width, 3m height, a 1:1.5 side slope, and a longitudinal slope of 15 cm/km. The canal is lined by using smooth concrete with a Manning roughness of 0.015. The canal bed and top levels are 14.8 and 17.8 m.a.m.s.l., respectively. The water level at station zero of the canal reaches 16.8 m.a.m.s.l.

To examine its hydraulic performance, a physical model was constructed according to the basic design drawings of the stilling basin of Taziz Al-Taziz pumping station by The Center of Studies and Engineering Designs of the Iraqi Ministry of Water Resources, **Fig. 2** shows the model setup that was carefully designed to reflect the characteristics of the stilling basin and part of the main canal. The model scale was chosen to be 1:16.

Figure 2. The physical model is installed in the laboratory of **(Center of Studies and Engineering Designs, 2024).**

During a site visit to the Taziz Al-Taziz pumping station, as shown in **Fig. 3,** it was found that its stilling basin doesn't match the basic design. Some modifications were made to the basic design. The design stilling basin was merged with a stilling basin of an old, demolished pumping station.

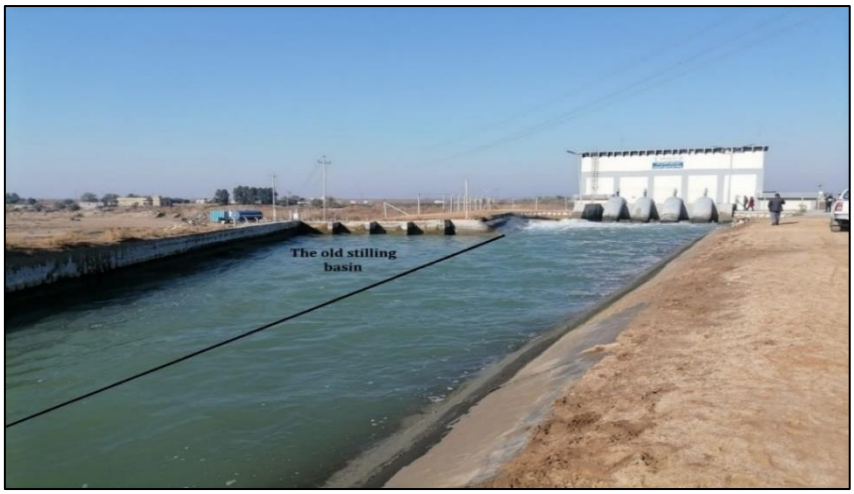

Figure 3. A view of the Taziz Al-Taziz pump station.

A survey team conducted a field measurement to obtain as-built dimensions of the stilling basin, as shown in **Fig. 4.**

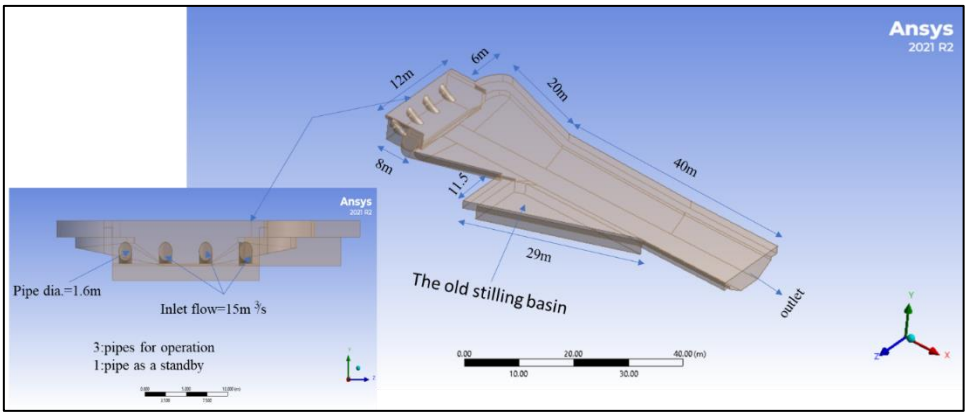

Figure 4. As built geometry.

3. VELOCITY MEASUREMENTS CONDUCTED ON THE PHYSICAL MODEL

An electromagnetic velocity measurement device was used to measure the flow velocity across the flow path at the upstream side of the canal of the physical model. It is 75cm from the downstream end of the stilling basin in the model. This equals 12 m in the prototype. The measurements were conducted under consistent conditions, with the total water depth maintained at 12.5 cm, and this depth equal to 2 m in the prototype.

Table 1 lists the velocity profiles that were recorded in the model and the calculated prototype velocities. The velocity in the model was recorded at different depths across the section at three locations. Left side at a distance of 3cm from the left side wall, center, and right at a distance of 3cm from the right side wall of the section. The subscripts m and p refer to the model and the prototype, respectively.

Table 1. Velocity Profile at the beginning of the Canal.

Depth, cm		Velocity at the left side		Velocity at the center		Velocity at the right side	
$d_{m(cm)}$	$d_{p(m)}$	$v_{m(cm/s)}$	$v_{p(m/s)}$	$v_{m(cm/s)}$	$v_{p(m/s)}$	$v_{m(cm/s)}$	$v_{p(m/s)}$
2.5	0.4	0.28	1.12	0.29	1.16	0.25	1
5	0.8	0.26	1.04	0.31	1.24	0.27	1.08
7.5	1.2	0.23	0.92	0.31	1.24	0.29	1.16
10	1.6	0.23	0.92	0.34	1.36	0.33	1.32

4. STRATEGY OF ANSYS PROGRAM

This study is focused on developing a detailed and comprehensive mathematical model that integrates the Navier-Stokes equations to describe the flow mechanics within the hydraulic system effectively, which combines pressure and velocity techniques with an emphasis on pressure-based and momentum-coupled algorithms and by incorporating well-established turbulence models, such as the Realizable k-ε because it provides better predictions in situations with significant turbulence, such as near walls or in curved geometry **(Darwish and Moukalled, 2009; Fluent, 2011; Yousif et al., 2015; Shaheed and Azzubaidi, 2022)** as a model, and for multiphase flow using volume of fluid VOF. **(Fluent, 2011; Alwan and**

Azzubaidi, 2021; Alsarefi and Azzubaidi, 2021; Azeez and Azzubaidi, 2022). The research aims to provide an accurate representation of the turbulent flow phenomenon within the stilling basin, and these turbulence models are essential for capturing the complex behaviors of fluid flow, particularly in environments where turbulence plays a significant role**. Fig.5** shows the CFD process presented by **(Zuo, 2005).**

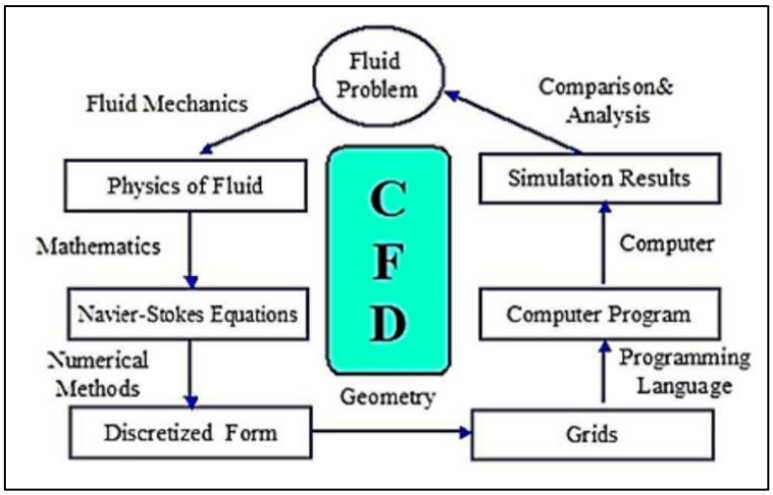

Figure 5. Flowchart showing the CFD process**. (Zuo, 2005)**.

4.1 Equations and Tools used in ANSYS Fluent

An essential element for achieving effective design and ensuring sustainable management of water resources and the Navier-Stokes and continuity equations are numerically solved using the finite volume method FVM equation these equations are a derivative **(Ashgriz and Mostaghimi, 2002; Biringen and Chow, 2011; Date, 2012; Yang et al., 2017)**, mass conservation law for flowing fluids, and Newton's second law. According to the governing equation for Ansys Fluid can be expressed as follows: Navier-Stokes equations:

$$\rho\left(\frac{\partial u}{\partial t}+u\frac{\partial u}{\partial x}+v\frac{\partial v}{\partial y}+w\frac{\partial w}{\partial z}\right)=\mu\left(\frac{\partial^2 u}{\partial x^2}+\frac{\partial^2 u}{\partial y^2}+\frac{\partial^2 u}{\partial z^2}\right)+\rho g_x-\frac{\partial p}{\partial x} \quad (1)$$

$$\rho\left(\frac{\partial v}{\partial t}+u\frac{\partial u}{\partial x}+v\frac{\partial v}{\partial y}+w\frac{\partial w}{\partial z}\right)=\mu\left(\frac{\partial^2 v}{\partial x^2}+\frac{\partial^2 v}{\partial y^2}+\frac{\partial^2 v}{\partial z^2}\right)+\rho g_y-\frac{\partial p}{\partial y} \quad (2)$$

$$\rho\left(\frac{\partial w}{\partial t}+u\frac{\partial u}{\partial x}+v\frac{\partial v}{\partial y}+w\frac{\partial w}{\partial z}\right)=\mu\left(\frac{\partial^2 w}{\partial x^2}+\frac{\partial^2 w}{\partial y^2}+\frac{\partial^2 w}{\partial z^2}\right)+\rho z-\frac{\partial p}{\partial z} \quad (3)$$

Continuity equation:

$$\frac{\partial u}{\partial x}+\frac{\partial v}{\partial y}+\frac{\partial w}{\partial z}=0 \quad (4)$$

Where:
u, v, and w are the three-dimensional velocity components (m/s).
ρ is the density(kg/m^3).
μ is the dynamic viscosity (N.s/m^2).
P is the pressure, Pa.
g is the gravitational acceleration (m/s^2)
t: is the time (s).

The turbulent Kinetic Energy k (from the k–ϵ model) used for this model is as follows: **(Petrila and Trif, 2004; Date, 2005; Niyogi, 2006; Versteeg and Malalasekera, 2007; ANSYS Fluent Theory Guide, 2021; Sharma, 2021; Badr and Azzubaidi, 2023)**

$$\frac{\partial(\rho k)}{\partial t}+\frac{\partial}{\partial x_j}\left(\rho k u_j\right)=\frac{\partial}{\partial x_j}\{\frac{\mu_t}{\sigma_k}\frac{\partial k}{\partial x_j}\}+2\mu_t s_{ij}.s_{ij}-\rho\varepsilon \quad (5)$$

$$\frac{\partial}{\partial t}(\rho\varepsilon)+\frac{\partial}{\partial x_j}\left(\rho k u_j\right)=\frac{\partial}{\partial x_j}\{\frac{\mu_t}{\sigma_k}\frac{\partial k}{\partial x_j}\}+c_{1\varepsilon}\frac{\varepsilon}{k}2\mu_t s_{ij}.s_{ij}-c_{2\varepsilon}\rho\frac{\varepsilon^2}{k} \quad (6)$$

Where μt is the turbulent eddy viscosity modeled as:

$$\mu t = C\rho\theta l=\rho c_\mu\frac{k^2}{\varepsilon} \quad (7)$$

$$\frac{\mu_t}{\delta_k}=\mu+\frac{\mu_t}{\delta_k} \quad (8)$$

$$\frac{\mu t}{\delta_\varepsilon}=\mu+\frac{\mu_t}{\delta_\varepsilon} \quad (9)$$

Where l is the length scale, and v is the velocity scale

$$\theta=k^{1/2} \quad (10)$$

$$l=\frac{k^{3/2}}{\varepsilon} \quad (11)$$

$C\mu$, $C\varepsilon 1$, 2, δk, and $\delta\varepsilon$ are dimensionless constants, which have the following values:
$C\mu$ = 0.09, $C\varepsilon 1$ = 1.44, $C\varepsilon 2$ = 1.92, δk=1.0, $\delta\varepsilon$=1.30

$$s_{ij}=\frac{\partial U_i}{\partial x_j}+\frac{\partial U_j}{\partial x_i} \quad (12)$$

Where:
ui, = Velocities vectors, m/s.
xi, = Space dimensions, m.
K = Turbulent kinetic energy, m^2/s^2
ε = Turbulent dissipation rate, m^2/s^3

This simplified version of the model can be utilized to understand the equilibrium between the generation and dissipation of turbulent kinetic energy, and the turbulence kinetic energy equation, as formulated by **(Hanjalic and Launder, 1972)** provides a foundational approach for assessing the behavior of turbulence within fluid dynamics and this equation allows for the calculation of the energy associated with turbulent flow, which is crucial for evaluating the efficiency of energy dissipation in hydraulic structures such as stilling basins.

4.2 Computational Mesh Generation

In the process of modeling the stilling basin and canal, an accurate computational mesh was generated to ensure the precision of the simulations by using unstructured tetrahedral mesh, and the quality of the mesh was assessed using two important metrics in computational fluid dynamics CFD: skewness and orthogonality these metrics were carefully

evaluated to confirm that the mesh was of good quality, as indicated by the results and the following table outlines the quality ranges for skewness and orthogonality, color-coded for ease of interpretation as shown in **Fig. 6.** Mesh independence test was performed to ensure that the simulation results are not dependent on mesh size. Three different mesh densities were tested: coarse, medium, and fine. Key hydraulic variables such as velocity and pressure were compared at critical points within the stilling basin. The results showed a noticeable difference between the coarse and medium meshes, while the difference between the medium and fine meshes was negligible. This indicates that the numerical solution had reached mesh independence. Therefore, the medium mesh was selected for the remaining simulations to ensure a balance between accuracy and computational efficiency. The simulation was conducted with a highly refined mesh, containing over 11,10,13 million elements for design, as-built, and physical model, respectively, ensuring that the model accurately simulated the flow dynamics within the basin and canal and validating the model accuracy.

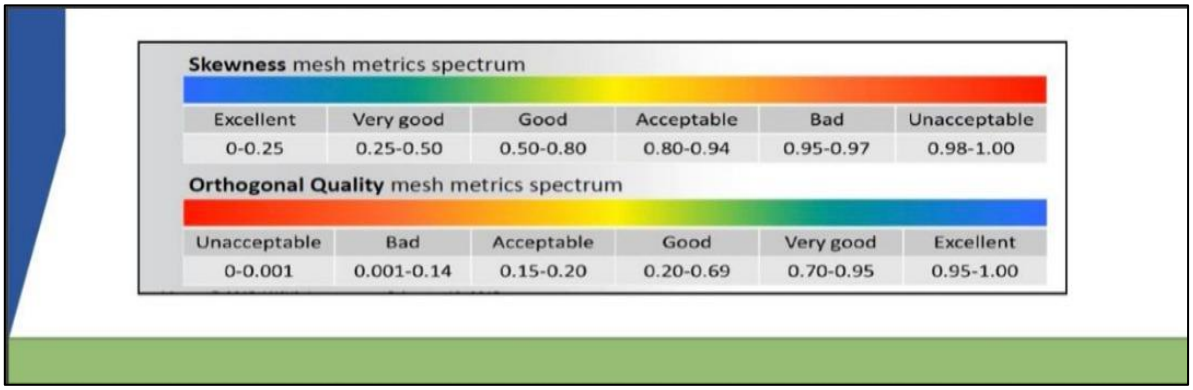

Figure 6. Mesh quality evaluation table.

4.3 Boundary Conditions

The conditions were incorporated to ensure the model could reflect practical scenarios, and these included specifying the water inlet velocity, outlet pressure, and the water level at the outlet, which were essential for defining the flow characteristics within the system. The turbulence intensity was estimated based on the inlet flow characteristics and basin geometry. A value of 5% was assigned, considering the influence of multiple inflow pipes and the presence of an end sill, both of which contribute to increased turbulence levels. Regarding wall roughness, it was modeled using the standard wall function approach by specifying two primary parameters: Roughness height and roughness constant.

5. RESULTS AND ANALYSES

The results of the investigations on the hydraulic performance of the basic design of Taziz Al-Taziz pumping station stilling basin, its physical model, and the as-built basin are presented in the following sections.

5.1 The Basic Design

Fig. 7 shows the flow streamlines and eddies that occur in the stilling basin. Most of the turbulence occurs within the stilling basin, and then turbulence begins to settle down at

almost 10 m from the downstream end of the basin, with an average velocity at this point in the canal equal to 1.4 m/s.

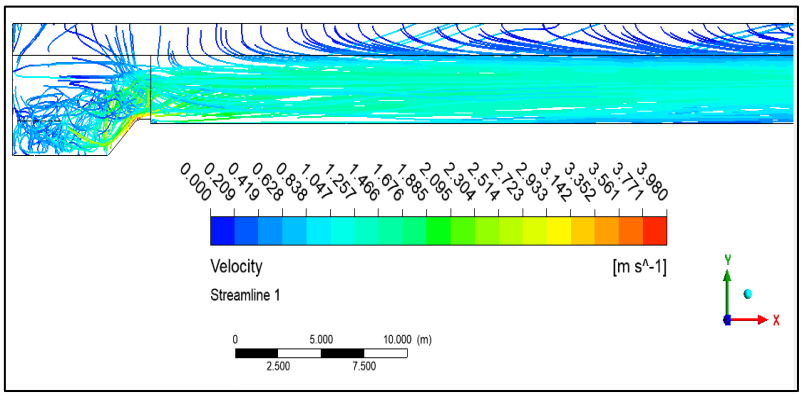

Figure 7. Velocity streamlines along the center line of the basic design.

Fig. 8 shows the velocity distribution within the basin when applying the Taziz Al-Taziz model's basic design. The velocity distribution varies between minimum values of 0.25 m/s to maximum values of 3.98 m/s. The velocity distribution shows that there are low velocity areas, as indicated by lower values such as 0.209, 0.419, 0.628, and 1.047m/s, and these values are often found in the outlet canal or at quiet corners before pipes close to the retaining wall, where the flow is less intense. The angle of the pipe openings, angle 36°, which directly affects the kinetic energy of the water as the outflowing water impacts the bottom of the canal, causing a significant drop in velocity.

As the velocity gradually increases up to intermediate values such as 1.257, 1.466, 1.676 and 1.885 m/s, it can be seen that these regions are located in the central regions of the basin or those where water interacts with the bed more clearly and these velocities show the flow response to the basin design, where the velocity is so distributed that the kinetic energy is transmitted without excessive turbulence.

At higher values, such as 2.095 to 3.98 m/s, these velocities are mainly concentrated above the sill end and near the entrance of the canal.

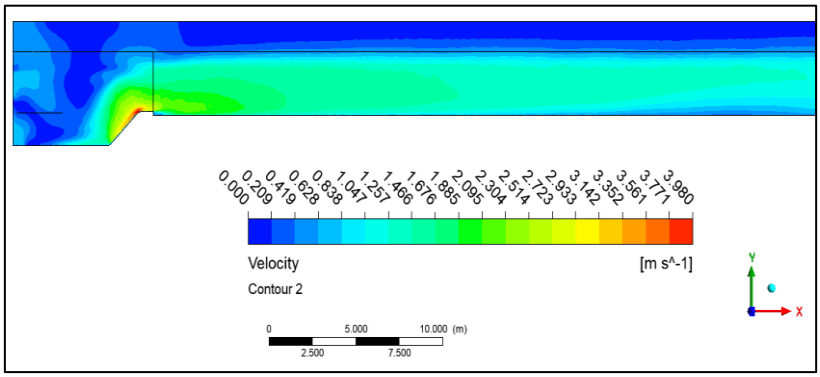

Figure 8. Velocity distribution along the center line of the basic design.

Fig. 9 shows that the pressure in water is affected by several factors, including the depth of the water, and the water that flows from the pipes leads to dynamic changes in pressure. When the water pushes forcefully from the pipes, a high momentum is generated due to its high velocity. Maximum pressure is at the largest depth, equal to 35042.738 Pa; the pressure decreases uniformly, reaching 2503.053 Pa near the surface.

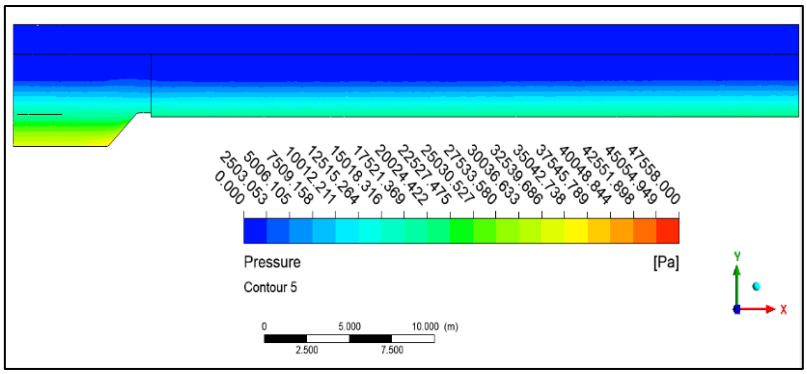

Figure 9. Pressure along the center line of the basic design of the stilling basin.

5.2 As Built

Fig. 10 shows the flow streamlines and eddies that occur in the stilling basin and shows the distance at which the flow begins to settle inside the canal, as it is approximately 30 m from the downstream end of the basin, with an average velocity at this point in the canal equal to 1 m/s.

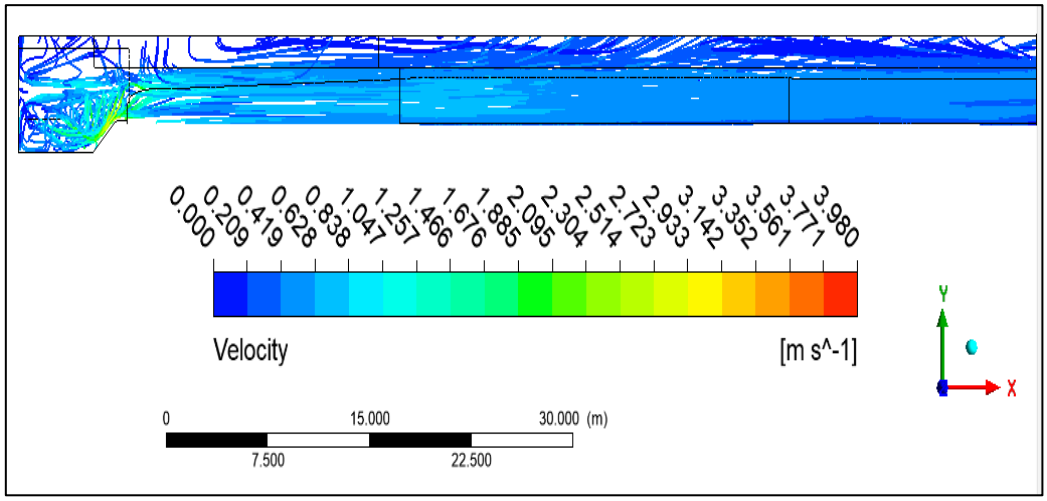

Figure 10. Velocity stream line along the center line of the as-built**.**

Fig. 11 illustrates the velocity distribution within the basin when applying the as-built Taziz Al-Taziz model. The velocity distribution range is approximately from the minimum values of 0.209 to the maximum values of 3 m/s. These values reflect significant variations in water velocity depending on depth and location within the basin. The low-velocity areas, 0.209 to 1.047 m/s, are found in the basin close to the retaining wall of pipes, where the flow is less intense, and the significant reduction in velocity in areas before the pipes can be explained by several engineering and dynamic factors influencing water flow within the basin.
As the velocity gradually increases up to intermediate values such as 1.257 to 2.304 m/s, it can be seen that these regions are located before and above the sill end of the basin where water interacts with it more clearly and these velocities show the flow response to the basin design, where the velocity is so distributed that the kinetic energy is transmitted without excessive turbulence.

At higher values, such as 2.514 to 2.98 m/s, these velocities are mainly concentrated on the sill end or in areas with strong currents, and these areas may indicate significant flow turbulence.

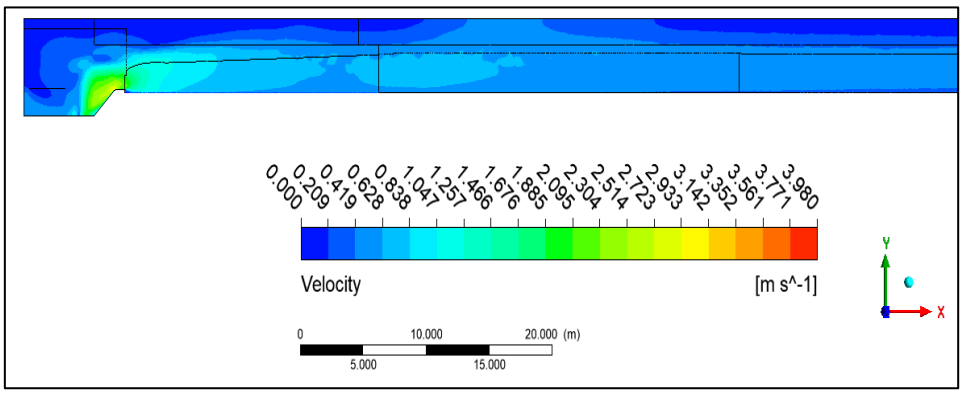

Figure 11. Velocity distribution along the center line of the stilling basin.

Fig. 12 shows that the maximum pressure is almost 40048 Pa at a greater depth of 5 m and gradually decreases uniformly until it reaches 2503 Pa.

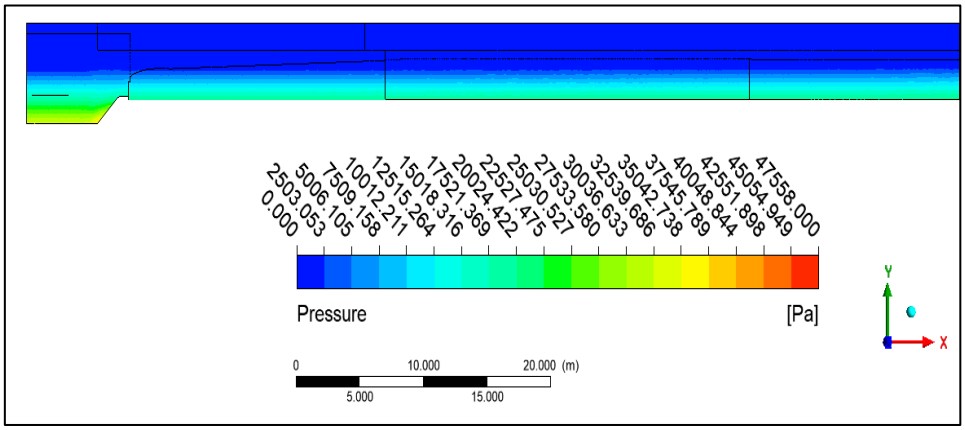

Figure 12. Pressure along the center line of as as-built stilling basin.

5.3 The Physical Model

Physical module runs were conducted to measure the flow velocity at a cross-section at the upstream side of the main canal at the design discharge and are shown in **Table 1.** **Fig. 13** shows the water flow distribution at the beginning of the canal obtained by applying the CFD model. The velocity reaches 0.442 m/s as a maximum value. This value is equal to 1.768 m/s in the prototype. Initially, areas with low velocities, such as 0.055 and 0.166 m/s equal to (0.22 and 0.664 m/s) in prototype, exhibit stable flow conditions, where water moves slowly, reducing the turbulence or erosion and these low-velocity regions are relatively safe from erosion this region appears in the left side of the section because the operation condition which includes operating three pipes from the right. As the velocity increases to intermediate values between 0.221 and 0.332 m/s equal to (0.884 to 1.328 m/s) in prototype in the middle of the section, the flow begins to show more movement, and in regions where the flow velocity exceeds 0.387 to almost 0.442 m/s equal to (1.548 to

1.768m/s) in prototype at the right of the section, high turbulence concentrations are observed caused by operating of three pipes.

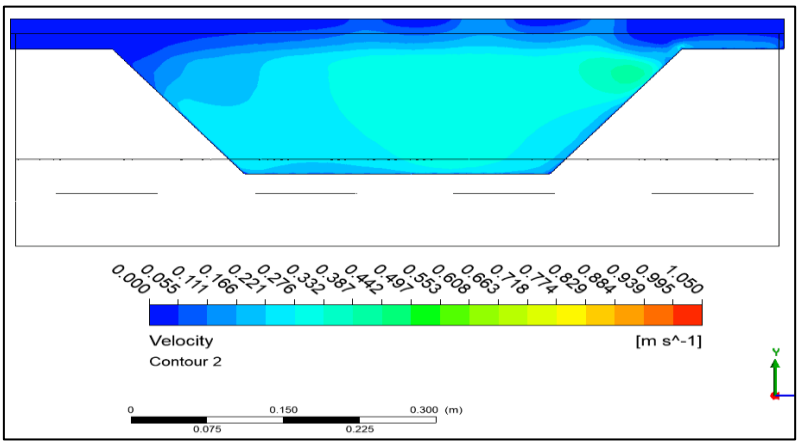

Figure 13. Cross-section of water velocity distribution at the beginning of the canal of the physical model.

Table 2 includes the measurements of velocity at the beginning of the canal with different depths (left side within 3 cm from the left side wall, center, and right side with 3cm from the right side wall). The highest velocity was recorded at the center of the canal, reaching 0.32 m/s at depths of 7.5 cm and 10 cm. This distribution reflects the effect of sidewall friction, as the velocity gradually decreases closer to the canal walls due to viscosity and shear forces. On the left and right sides, velocity decreases significantly compared to the center. The lowest recorded velocity was 0.21 m/s at 10 cm depth on the left side, while on the right side, the velocity was equal to 0.29 m/s at the same depth, possibly indicating asymmetry in the flow or secondary flow effect.

Table 2. Velocity distribution at the beginning of the Canal.

Depth		Velocity at the left side		Velocity at the center		Velocity at the right side	
$D_{m(cm)}$	$D_{p(m)}$	$v_{m(cm/s)}$	$v_{p(m/s)}$	$v_{m(cm/s)}$	$v_{p(m/s)}$	$v_{m(cm/s)}$	$v_{p(m/s)}$
2.5	0.4	0.26	1.04	0.27	1.08	0.23	0.92
5	0.8	0.23	0.92	0.29	1.16	0.25	1
7.5	1.2	0.22	0.88	0.32	1.28	0.26	1.04
10	1.6	0.21	0.84	0.32	1.28	0.29	1.16

The match percentage is calculated between the velocities of the physical model at the same depth and position (left, center, right) in the three sections of the canal (beginning, middle, and end) and the velocities of the mathematical model. The matching is 90%. This is a good agreement between the two models, reflecting the accuracy of CFD in representing real physical conditions. This confirms the reliability of the numerical model in simulating complex hydraulic and physical phenomena. Such an agreement reinforces the use of CFD as an effective tool for studying and analyzing engineering systems, particularly in cases where laboratory experiments are costly or impractical. Additionally, these findings support the potential of numerical models in predicting the future behavior of studied systems and optimizing their designs based on digital data analysis. **Fig. 14** shows the flow streamlines and eddies that occur in the stilling basin and shows the distance at which the flow begins to

settle inside the canal, as it is approximately 75 cm from the downstream end of the basin, and that is equal to 12 m at the prototype. The average velocity at this point in the canal is equal to 0.32 cm.

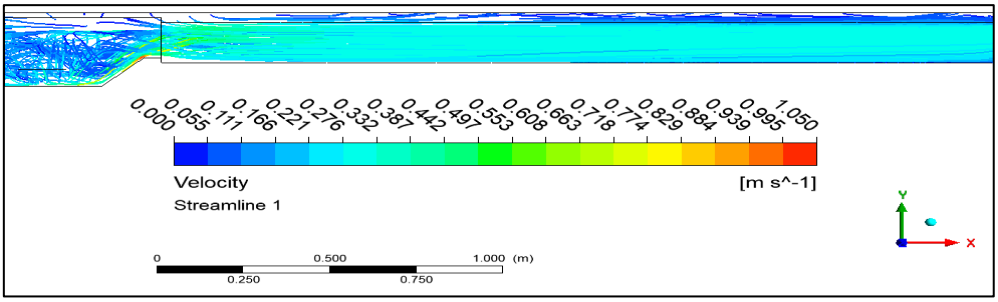

Figure 14. Velocity stream line along the center line of the physical model.

Fig. 15 shows the velocity distribution within the physical model of Taziz Al-Taziz, highlighting how velocity varies across different regions of the system. In areas with very low velocities close to 0.221 m/s as a maximum value, that is equal to 0.884 m/s in the basin, which is also considered one of the low velocity zones in the prototype, within the area close to the retaining wall of pipes. At higher velocity ranges 0.663 m/s to 1.05 m/s, which are equal to 2.652 m/s and 4.2 m/s, which are also considered one of the high velocity zones in the prototype, located at the sill end in the same prototype and model. This indicates that the model matches the prototype.

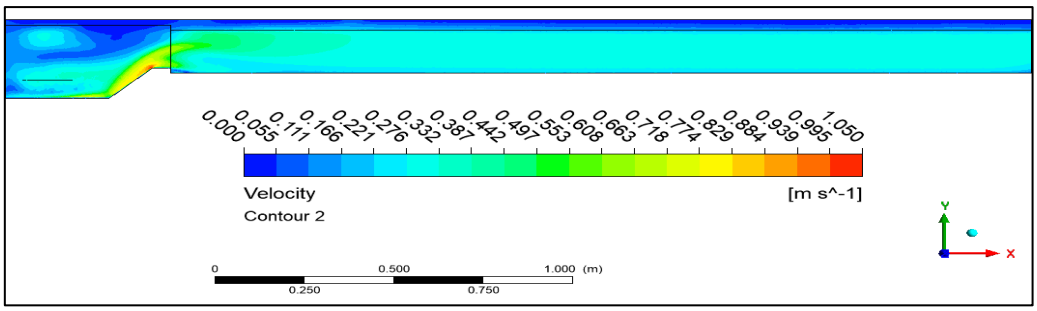

Figure 15. Velocity distribution along the center line of the physical model

Fig. 16 shows the pressure starting at 2467.0 Pa at the greatest depth, 30 cm, and gradually decreasing with decreasing depth until it reaches 129.843 Pa at the top. The relationship between pressure and depth is approximately linear because the weight of the water column decreases as depth decreases.

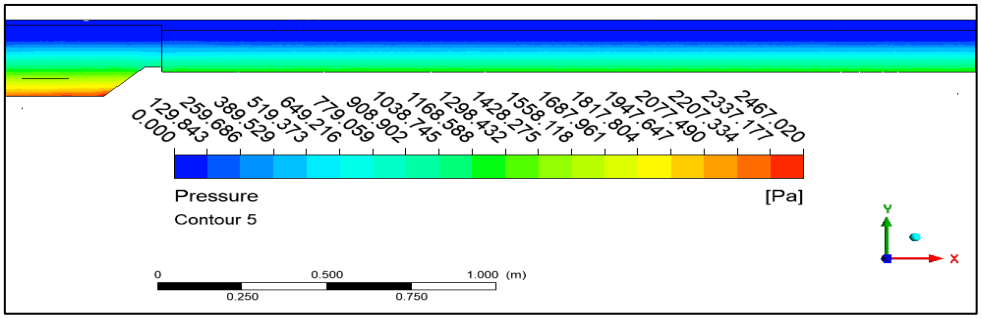

Figure 16. Pressure along the centerline of the Physical Model.

When comparing the numerical model to the physical model, several differences and limitations appear, most notably when creating a rigged physical model; the dimensions of the realistic phenomenon are reduced based on a specific scale. This causes several challenges, including the forces acting do not match accurately at small scales, such as surface tension influential than the real situation, which may lead to results that are not fully representative of reality. Also, the difficulty of achieving complete similarity (geometric and dynamic) at the same time affects the accuracy of results, and the cost and time required to build and operate a physical model require significant resources. The numerical model provides flexibility and speed, but is affected by quality and solution method. Both models have advantages and limitations, and it is preferable to use them together for cross-validation and improving prediction accuracy. The analysis of the canal velocity measurements and the hydraulic performance of the stilling basin at Taziz Al-Taziz pumping station represents two different yet complementary approaches to evaluating hydraulic flow behavior. While the canal velocity analysis focuses on direct velocity measurements at the beginning of the canal using an electromagnetic velocity measurement device, the stilling basin analysis utilizes CFD simulations to compare the basic design, physical model, and the as built configurations, and the canal velocity study measures flow velocity at three key locations: the beginning, middle, and end of the canal and the results indicate that velocity gradually decreases with depth due to frictional effects with the canal bed and walls, with the highest velocities recorded at the center.

6. EFFICIENCY OF THE STILLING BASINS

Based on the discharge, velocity of the water pipe outlet, the angle of inclination of the pipes, and the discharge and velocity of the water entering the canal, the efficiency of the stilling basins was calculated based on the momentum equation. It was found that the efficiency of the basic design stilling basin of the Taziz Al-Taziz pumping station is equal to 30.7% and 36.7% for the physical model stilling basin. This means that the quality of the basin in dissipating energy is poor, as the dimensions of the basin are insufficient to dissipate a large amount of energy. The calculated efficiency of the as-built was found to be equal to 50.5%. This indicates the quality and efficiency of the as-built Taziz Al-Taziz in dispersing a large percentage of the energy of the water emerging from the pipes. That is because the complementary to the stilling basin caused an additional dispersal of energy. Improved efficiency means a more uniform flow distribution and reduced high velocities or turbulent flow areas. This contributes to reducing the erosion of the canal bottom and sides. Thus, it reduces the need for ongoing maintenance and extends the life of the hydraulic infrastructure. When the efficiency increases, this means that the settling basin becomes better able to manage high water flow and reduce turbulence entering the canal. This leads to reducing operating and maintenance costs.

7. CONCLUSIONS

In this study, an engineering and modeling analysis of the stilling basin at the Taziz Taziz pumping station was conducted using SolidWorks software and Computational Fluid Dynamics CFD simulation through ANSYS, and the goal of the study is to evaluate the hydraulic performance of the system under investigation by studying the velocity and pressure distributions within the basin and the surrounding canal and identifying areas that may experience flow disturbances or structural erosion and the approach involves using a

combined mathematical model with the Navier-Stokes equations and turbulence models such as the k-ε model to understand the dynamic behavior of fluids and achieve efficient and sustainable designs and the results indicate that:

1. Streamlines begin to settle at a distance of 10m in the canal from downstream of the stilling basin in the basic design and at 10 m in the canal within 30m from downstream of the stilling basin in the as-built. And 75cm in the physical model is equal to 12m in the prototype.
2. It was found a decrease in velocity was found from 3.980 m/s in the basin to 1.4 m/s in the canal, 3 m/s to 1 m/s in the basic design, and as built, respectively. By converting the physical model velocity to the prototype, the decrease in velocity is from 4.2 m/s to 1.28 m/s.
3. It was found that there is no negative pressure, indicating that the pressures within the structure are stable and that values less than atmospheric pressure are not reached.
4. The matching percentage is 90% between the CFD physical model and the laboratory model.
5. Efficiency of the stilling basin is equal to 30.7% and 36.7%, and 50.5% for the basic design, physical model stilling basin, and as built, respectively.

Acknowledgments

This work was supported by the Water Resource Engineering Department, University of Baghdad.

Credit Authorship Contribution Statement

Arafh Fadhel Albayati: Writing – review & editing, original draft, Validation, Software, Methodology. Riyadh Z. Azzubaidi: Supervision, Conceptualization, review & editing.

Declaration of Competing Interest

The authors declare that they have no known competing financial interests or personal relationships that could have appeared to influence the work reported in this paper.

REFERENCES

Abed, B. S., and Majeed, H. Q., 2020. The behavior of scouring around multiple bridge piers having different shapes. *IOP Conference Series: Materials Science and Engineering*, 745(1), P. 012158. IOP Publishing. https://doi.org/10.1088/1757-899X/745/1/012158.

Abood, M. S., Hussain, I., and Ali, A. H. A., 2025. Theoretical and experimental investigation of the effects of inverted wings modifications on the stability and aerodynamic performance of a sedan car at cornering. *Engineering Reports*, e13026, 7(1), P. 27. https://doi.org/10.1002/eng2.13026.

Aboulatta, N., Ezizah, G., Yousif, N. and Fathy, S., 2011. Design of stilling basins using artificial roughness. *International Journal of Civil and Environmental Engineering*, 3(2), pp. 65-71.

AL, A. M. H., and Azzubaidi, R. Z., 2021. Investigations on the impact of using elliptic groynes on the flow in open channels. *Journal of Engineering*, 27(2), pp. 44-58. https://doi.org/10.31026/j.eng.2021.02.04.

Aleyasin, S. S., Fathi, N., and Vorobieff, P., 2015. Experimental study of the type VI stilling basin performance. *Journal of Fluids Engineering*, 137(3), P. 12. https://doi.org/10.1115/1.4029164.

Alwan, I. A., and Azzubaidi, R. Z., 2021. A computational fluid dynamics investigation of using large-scale geometric roughness elements in open channels. *Journal of Engineering*, 27(1), pp. 35-44. https://doi.org/10.31026/j.eng.2021.01.03.

Ashgriz, N., and Mostaghimi, J., 2002. An introduction to computational fluid dynamics. Fluid flow handbook, 1, Ch. 4, pp. 1-49.

ANSYS Fluent Theory Guide, Release 21.0, ANSYS, Inc. 2600 ANSYS Drive, Canonsburg, PA 15317, January 2021.

Azeez, M.H., Azzubaidi, R.Z., 2022. Flow over the spillway of aladhiam dam under gated conditions. *Journal of Engineering*, 28(11), pp. 107-123. https://doi.org/10.31026/j.eng.2022.11.08.

Babaali, H., Shamsai, A. and Vosoughifar, H., 2014. Computational modeling of the hydraulic jump in the stilling basin with convergence walls using cfd codes. *Arabian Journal for Science and Engineering*, 40(2), pp. 381-395. https://doi.org/10.1007/s13369-014-1466-z.

Babaali, H., Soori, N., Soori, S., Mojtahedi, A., and Hamedi, A., 2018. Static pressure estimation on converging USBR II stilling basin: numerical approach. *International Journal of Science and Engineering Investigations*, 7(79), pp. 97-89.

Badr, S. H., and Azzubaidi, R. Z., 2023. Using CFD modeling to simulate the control of the propagation of salt wedge using inclined roughness elements. E3S Web of Conferences, 427 (04008). P. 9. https://doi.org/10.1051/e3sconf/202342704008.

Behnamtalab, E., Maskani, V., and Sarkardeh, H., 2023. Numerical study of turbulent flow in USBR VI stilling basin. Applied Water Science. 13(7), P. 146. https://doi.org/10.1007/s13201-023-01956-9.

Biringen, S. and Chow, C.Y., 2011. *An introduction to computational fluid mechanics by example*. John Wiley & Sons.

Center of Studies and Engineering Designs, 2024. Collected data from various projects in the ministry of water resources in Iraq.

Darwish, M., Sraj, I. and Moukalled, F., 2009. A Coupled finite volume solver for the solution of incompressible flows on unstructured grids. *Journal of Computational Physics*, 228(1), pp. 180-201. https://doi.org/10.1016/j.jcp.2008.08.027.

Date, A.W., 2005. *Introduction to computational fluid dynamics.* Cambridge University Press.

Date, A.W., 2012. *Introduction to computational fluid dynamics*. Cambridge University Press.

Goel, A. R. U. N., 2007. Experimental study on stilling basins for square outlets. *In the 3rd WSEAS International Conference on Applied and Theoretical Mechanics,* Spain. pp. 157-162.

Hanjalic, K. and Launder, B.E., 1972. A Reynolds stress model of turbulence and its application to thin shear flows. *Journal of Fluid Mechanics*, 52, pp. 609-638. https://doi.org/10.1017/S002211207200268X.

Kadhim, A. F. and Al Thamiry, H. A., 2020. Computation of critical submergence depth to avoid surface vortices at vertical pump intakes. *Journal of Engineering*, 26(8), pp. 59-68. https://doi.org/10.31026/j.eng.2020.08.05.

Lu, L., Li, Y.C., Teng, B. and Chen, B., 2008. Numerical simulation of turbulent free surface flow over an obstruction. *Journal of Hydrodynamics*, 20(4), pp. 414-423. https://doi.org/10.1016/S1001-6058(08)60075-X.

Majeed, H. Q., and Ghazal, A. M., 2020. CFD simulation of velocity distribution in a river with a bend cross-section and a cubic bed roughness shape. *IOP Conference Series: Materials Science and Engineering*, 928(2), P. 022038. IOP Publishing. https://doi.org/10.1088/1757-899X/928/2/022038.

Mohammed, S. R., Nile, B. K., and Hassan, W. H., 2020. Modelling stilling basins for sewage networks. *In IOP Conference series: Materials Science and Engineering*, 671(1), P. 012111. https://doi.org/10.1088/1757-899X/671/1/012111

Niyogi, P., 2006. *Introduction to Computational Fluid Dynamics*. Pearson Education India.

Peterka, A.J., 1964. Hydraulic design of stilling basins and energy dissipators. United States Department of the Interior. No. 25. Bureau of Reclamation.

Petrila, T., and Trif, D., 2004. Basics of fluid mechanics and introduction to computational fluid dynamics, 3. *Springer Science and Business Media*.

Salman, S. D., Kadhum, A. A. H., Takriff, M. S., and Mohamad, A. B. 2013. CFD simulation of heat transfer and friction factor augmentation in a circular tube fitted with elliptic-cut twisted tape inserts. *Mathematical Problems in Engineering*, 163839. 2013 (1), P .11. https://doi.org/10.1155/2013/163839.

Shaheed, A. K., and Azzubaidi, R. Z., 2022. CFD simulation model of salt wedge propagation. *Journal of Engineering*, 28(1), pp. 76-85. https://doi.org/10.31026/j.eng.2022.01.06.

Sharma, I., Mishra, A., and Mehrotra, R., 2021. Performance evaluation of the impact stilling basin using ANSYS Fluent. *In Advances in Water Resources and Transportation Engineering: Select Proceedings of TRACE 2020*, pp. 139-149. Springer Singapore. http://dx.doi.org/10.1007/978-981-16-1303-6_11.

Soori, S., Babaali, H. and Soori, N., 2017. An optimal design of the inlet and outlet obstacles at USBR II Stilling Basin. *International Journal of Science and Engineering Applications*, 6(5), pp. 134-142. http://dx.doi.org/10.7753/IJSEA0605.100.

Tabatabai, M., Heidarnejad, M. and Bordbar, A., 2014. Numerical study of flow patterns in a stilling basin with a sinusoidal bed using the flow 3D Model. *Advances in Environmental Biology*, 8(13), pp. 787-792.

Valero, D., Bung, D., Crookston, B.M., and Matos, J., 2016. Numerical investigation of USBR type III stilling basin performance downstream of smooth and stepped spillways. *6th IAHR International Symposium on Hydraulic Structures,* Portland, OR, 27-30 June pp. 652-663 https://doi.org/10.15142/T340628160853.

Verma, D.V.S. and Goel, A., 2003. Development of efficient stilling basins for pipe outlets. *Journal of Irrigation and Drainage Engineering*, 129(3), pp. 194-200. https://doi.org/10.1061/(ASCE)0733-9437(2003)129:3(194).

Versteeg, H. K., and Malalasekera, W., 2007. *An introduction to computational fluid dynamics: the finite volume method*, 2nd ed., Pearson Education, Limited, London, England.

Xiong, Q., Yang, Y., Xu, F., Pan, Y., Zhang, J., Hong, K., Lorenzini, G., and Wang, S., 2017. Overview of computational fluid dynamics simulation of reactor-scale biomass pyrolysis. ACS Sustainable Chemistry & Engineering, 5(4), pp. 2783-2798. https://doi.org/10.1021/acssuschemeng.6b02634.

Yousif, A. H., Aljanabi, W. A. S., and Mahdi, A. M., 2015. Dynamic analysis of fluid–structure interaction of axial fan system. *Journal of Engineering,* 21(09), pp. 150-168. https://doi.org/10.31026/j.eng.2015.09.10.

Zaffar, M.W. and Hassan, I., 2023. Hydraulic investigation of stilling basins of the barrage before and after remodeling using FLOW-3D. Water Supply, 23(2), pp. 796-820. https://doi.org/10.2166/ws.2023.032.

Zuo, W., 2005, Introduction of computational fluid dynamics. Friedrich- Alexander-Universität Erlangen-Nürnberg.

تحليل أداء حوض التسكين في محطة ضخ تعزيز التعزيز في محافظة المثنى، العراق

عرفه فاضل البياتي*، رياض زهير الزبيدي

هندسه الموارد المائيه, كلية الهندسة ,جامعه بغداد, بغداد,العراق

الخلاصه

تمت دراسة محطة ضخ ري تعزيز التعزيز الواقعه في محافظة المثنى في العراق بهدف معرفة أداء حوض التسكين الخاص بها في تقليل طاقة المياه الخارجة من مخارج أنابيب التصريف. اعتمدت الدراسة على نتائج النموذج الفيزيائي للتصميم الأساسي لحوض التسكين واستخدام برنامج ANSYS Fluent 21.0 لمحاكاة كل من التصميم الأساسي وحوض التسكين المبني في ارض الواقع. تم تصميم وتنفيذ ودراسة النموذج الفيزيائي من قبل مركز الدراسات والتصميمات الهندسية التابع لوزارة الموارد المائية العراقية. أظهرت عمليات المحاكاة تباين السرعة ضمن التصميم الأساسي لمحطة ضخ تعزيز تعزيز من 3.98 م/ث إلى 0.209 م/ث في حوض التسكين بمتوسط سرعة في بداية القناة 1.4 م/ث. وبالنسبة لما تم بناءه على ارض الواقع لتعزيز التعزيز فقد أظهرت نتائج السرعة تباينا من 3 م/ث إلى 0.209 م/ث داخل الحوض بمتوسط سرعة 1 م/ث في بداية القناة. وبتحويل نتائج النموذج الفيزيائي المقاسة إلى نموذج أولي، أتضح أن متوسط السرعة في بداية القناة 1.28 م/ث. تبلغ كفاءة حوض التسكين بالتصميم الأساسي 30.7%، في حين تبلغ نسبة كفاءة النموذج المبني 50.5% و36.7% للنموذج الفيزيائي. وهذا يدل على جودة وكفاءة حوض التسكين المبني في تشتيت نسبة كبيرة من الطاقة المائية من الأنابيب. علاوة على ذلك، لم يتكون أي ضغط سلبي داخل الأحواض.

الكلمات المفتاحية: حوض التسكين، برنامج ANSYS، التصميم الهيدروليكي، توزيع السرعة، محطة الضخ، الخوارزميات المقترنة.